ELSEVIER

Journal of Photochemistry and Photobiology A: Chemistry 153 (2002) 11–18

Journal of Photochemistry and Photobiology A:Chemistry

www.elsevier.com/locate/jphotochem

Potentialities of diffuse reflectance laser-induced techniques in solid phase: A comparative study of benzophenone inclusion within *p-tert*-butylcalixarenes, silicalite and microcrystalline cellulose

L.F. Vieira Ferreira [a,*], M.R. Vieira Ferreira [b], A.S. Oliveira [a], J.C. Moreira [c]

[a] *Centro de Química-Física Molecular-Complexo Interdisciplinar, Instituto Superior Técnico, Av. Rovisco Pais, 1049-001 Lisboa, Portugal*
[b] *Secção de Química Orgânica, Departamento de Engenharia Química, Instituto Superior de Engenharia de Lisboa, R. Conselheiro Emídio Navarro, 1949-014 Lisboa, Portugal*
[c] *Centro de Estudos da Saúde do Trabalhador e Ecologia Humana, ENSP, Fundação Oswaldo Cruz, Rua Leopoldo Bulhões 1480, Rio de Janeiro RJ 21041-210, Brazil*

Received 17 June 2002; received in revised form 21 June 2002; accepted 12 July 2002

Abstract

Diffuse reflectance and laser-induced techniques were used to access photochemical and photophysical processes in solid phases, namely calix[*n*]arenes (*n* is the number of phenolic units in the ring), organic substances which are capable of forming inclusion complexes with several neutral organic substances and metal ions. We have used *p-tert*-butylcalix[4], *p-tert*-butylcalix[6] and *p-tert*-butylcalix[8]arenes as solid matrixes and benzophenone as probe. A comparative study is presented here, mainly using the results obtained with the calix[6]arene as host and those obtained with two other electronically inert supports: microcrystalline cellulose and silicalite, a hydrophobic zeolite.

In all substrates, room temperature phosphorescence was obtained in air equilibrated samples. The decay times vary greatly and the largest lifetime was obtained for silicalite, where benzophenone is included into hydrophobic channels. Calix[6]arene and cellulose provide full protection against oxygen quenching while silicalite only protects the guest molecule partially.

Calixarene molecules provide larger hydrophobic cavities than silicalite and also a better selectivity towards the guest size. This selectivity does not exist in the microcrystalline cellulose case.

FTIR absorption spectra show that the distortion from planarity in the benzophenone molecule is larger in silicalite than in calix[6]arene, while in cellulose the distortion is slight. In spite of this, benzophenone exhibits the highest phosphorescence emission quantum yield in the case of silicalite.

Benzophenone ketyl radical formation occurs with entrapment in cellulose and also with inclusion in calix[6]arene and calix[8]arene while in silicalite only triplet–triplet absorption is detected.

Keywords: Calixarenes; Silicalite; Microcrystalline cellulose; Benzophenone; Inclusion complexes; Diffuse reflectance; Flash photolysis; Room temperature phosphorescence

1. Introduction

The understanding of photochemical and photophysical processes involving a great variety of compounds included in solids has, recently, greatly improved as a consequence of both methodological advances and availability of new solid phases [1–4].

In solid state, photochemical methods have been applied to the study of several organic compounds adsorbed or included in many solid powdered substrates such as microcrystalline cellulose, silicalite, silicas, cyclodextrins and clays. The properties and applications of such solid substrates are described elsewhere [1–3].

Owing to their characteristics and selectivity, calixarenes appear to be an useful support material for photochemical studies. Calix[*n*]arenes (mainly those with $n = 4$, 6 and 8) have recently received considerable interest due to their ability to form inclusion complexes with organic molecules and ions in both water and organic solvents [5–16]. Many derivatives of calixarenes can recognise metal ions and neutral organic molecules with reasonable selectivity and for this reason they have been used in many areas such as catalysis, separation and analysis [17–21].

* Corresponding author. Tel.: +351-21-8419252; fax: +351-21-8464455.
E-mail address: luisfilipevf@ist.utl.pt (L.F. Vieira Ferreira).

1010-6030/02/$ – see front matter
PII: S1010-6030(02)00302-7

Calix[*n*]arene structure involves a cyclic array of *n* phenol moieties linked by methylene groups. Conformational isomerism in calixarenes has been reported [22–24]. In solution, *p-tert*-butylcalix[4]arene can adopt four conformations (conformers) called cone, partial cone, 1,2 alternate or 1,3 alternate. Cone conformation is the most stable in the solid state. This conformation presents a polar, hydrophilic part (OH rim) and a non-polar hydrophobic part (aromatic cavity) facilitating interactions with ions and neutral organic molecules. *p-tert*-Butylcalix[6]arene possesses eighth conformers and *p-tert*-butylcalix[8]arene, 16 conformers. These conformers are interconvertible in solution but for some cases some structures are favoured. For example, *p-tert*-butylcalix[4]arene exists mainly as cone conformation possessing all hydroxyl groups directed to the lower rim of the macrocycle and linked by an array of hydrogen bonds. Solvents such as acetone, acetonitrile and pyridine can increase the molecular mobility by destroying these hydrogen bonds [19].

Some inorganic ions are able to react with the phenolic oxygens [12]. The aromatic cavity is also able to "accommodate" guest species, in some cases, co-ordinating to guest molecule via π electrons [12].

The ability of calixarenes to form inclusion complexes, accommodating guest molecules or ions in their intramolecular cavities, greatly depends on the size and geometry of both guest molecule and host cavity [25–27]. As expected, the size of calixarenes cavities depends on the number of phenolic groups present in the calixarene molecule. In fact, experiments carried out with some polycyclic aromatic hydrocarbons possessing different dimensions and *p*-(diallylaminomethyl)calixarenes and *p*-(carboxyethyl)-calixarenes showed that calix[4]arenes are too small to accept naphthalene and calix[8]arenes apparently are too small to accept coronene and decacyclene but sufficient to accommodate durene, naphthalene, anthracene, phenanthrene, fluoranthene, pyrene and perilene [26]. Typical dimensions for the hydroxylic ring (lower rim) in the calixarene molecules measured using CPK molecular models varied from ca. 2.0 to 11.7 Å [26]. The capability of calix[*n*]arenes to form inclusion complexes with several organic compounds and inorganic ions has been reviewed [18,19,28,29].

In spite of the extended use of this family of compounds as hosts for inclusion complex formation, calixarenes have received much less attention from photochemists when compared with other host molecules of practical importance, even in solution studies. Very few photochemical studies of organic compounds within calixarenes were presented [30–35].

Silicalite is a de-aluminated analogue of ZSM-5 zeolite. The lack of substitutional aluminium results in silicalite having no catalytic or exchange properties, compared with the ZSM-5 zeolites. Silicalite is the only known hydrophobic form of silica and is capable of adsorbing organic molecules up to about 6 Å of kinetic diameter, even removing them from water [36].

Microcrystalline cellulose is an interesting powdered solid support with the remarkable property of protecting adsorbed probes from oxygen action [1,37,38]. Adsorption of probes on microcrystalline cellulose can be achieved by the use of a solution of the probe (e.g. benzophenone) and polar protic (e.g. alcohols) or aprotic (e.g. acetonitrile, acetone, dioxane) solvents. When the solid substrate is added to this solution, cellulose to cellulose hydrogen bonds are replaced by cellulose to solvent bonds and the matrix exhibits a certain degree of swelling which depends on the solvent used for sample preparation [37,38]. Probes can then penetrate within the polymer chains and stay entrapped after solvent removal.

Ground-state diffuse reflectance absorption spectroscopy, time resolved laser-induced luminescence and diffuse reflectance laser flash-photolysis are relatively new techniques that can be applied to study opaque and crystalline systems. By the use of these techniques, transient absorption and emission, triplet–triplet energy transfer, electron and hydrogen transfer can be accessed, as well as the nature of adsorption process and also the effect of solid host matrix on photo-induced processes [1–3,30,37–44].

This paper will present some potentialities of applying diffuse reflectance and laser-induced fluorescence to the study of benzophenone (BZP) included into *p-tert*-butylcalix[6]arene. These results will be compared with those obtained with other hosts, namely silicalite and microcrystalline cellulose.

2. Experimental

2.1. Materials

Benzophenone (Koch Light, purissimum), *p-tert*-butylcalix[4]arene, *p-tert*-butylcalix[6]arene and *p-tert*-butylcalix[8]arene (Aldrich) were used without any purification. Chloroform, isooctane and ethanol (Merck, Uvasol grade) were also used as received. Silicalite was from Union Carbide and cellulose was purchased from Fluka (Microcrystalline cellulose Fluka DS0).

2.2. Sample preparation

The samples used in this work were prepared using the solvent evaporation method. This method consists of the addition of a solution containing the probe to the previously dried or thermally activated powdered solid substrate, followed by solvent evaporation from the slurry in a fume cupboard. The final solvent removal was performed overnight in an acrylic chamber with an electrically heated shelf (Heto, Model FD 1.0–110) with temperature control ($25 \pm 1\,^{\circ}C$), under moderate vacuum at a pressure of ca. 10^{-3} Torr. The evaluation of the existence of final traces of solvent was monitored by the use of FTIR spectra.

For calixarenes, the solid complexes ketone/calixarene of molar ratios 1:1, 1:2.5 and 1:5 were prepared by mix-

ing a saturated solution of the calixarene in chloroform ($\sim 10^{-2}$ M of *p-tert*-butylcalix[4], *p-tert*-butylcalix[6] and *p-tert*-butylcalix[8]arenes) and a saturated solution of the ketone in the same solvent. The resulting mixture was magnetically stirred for at least 24 h and then allowed to evaporate in a fume cupboard until a completely dried sample was obtained. Finally, the complexes were dried under reduced pressure.

For silicalite samples, benzophenone selective adsorption into the silicalite channels was achieved using isooctane, whose molecular dimensions prevent this solvent to penetrate into the host channels. Following the initial solvent evaporation, samples were washed three times with isooctane for complete removal of the non-included ketone and dried again as described. Ground state absorption studies revealed that for 100, 250 and 500 μmol g^{-1} samples, the amount of ketone deposited onto silicalite surface does not exceed 20%.

For microcrystalline cellulose as host, samples were prepared with ethanol as described in detail in [37,38]. This solvent swells the cellulose matrix and benzophenone molecules become entrapped within the cellulosic polymer chains as studied before [1,37].

2.3. Methods

2.3.1. Ground state diffuse reflectance absorption spectra

Ground state absorption spectra for the solid samples were recorded using an OLIS 14 spectrophotometer with a diffuse reflectance attachment. Further details are given elsewhere [1,38].

2.3.2. Diffuse reflectance laser flash photolysis (DRLFP) system and laser-induced luminescence (LIL)

Schematic diagrams of the LIL system and of the DRLFP systems are presented in [1,39]. Laser flash photolysis experiments were carried out with the third harmonic of a YAG laser (355 nm, ca. 6 ns FWHM, ~10–30 mJ/pulse) from B.M. Industries (Thomson-CSF), model Saga 12-10, in the diffuse reflectance mode [1,30]. The light arising from the irradiation of solid samples by the laser pulse is collected by a collimating beam probe coupled to an optical fibre (fused silica) and is detected by a gated intensified charge coupled device (ICCD, Oriel model Instaspec V). The ICCD is coupled to a fixed imaging compact spectrograph (Oriel, model FICS 77440). The system can be used either by capturing all light emitted by the sample or in a time-resolved mode by using a delay box (Stanford Research Systems, model D6535). The ICCD has high speed (2.2 ns) gating electronics and intensifier and works in the 200–900 nm wavelength range. Time-resolved absorption and emission spectra are available in the nanosecond to second time range [1,30]. Transient absorption data are reported as percentage of absorption (% Abs.) defined as $100\Delta J_t/J_0 = (1 - J_t/J_0)100$, where J_0 and J_t are diffuse reflected light from sample before exposure to the exciting laser pulse and at time t after excitation, respectively [1,30]. For the LIL experiments a N_2 laser (PTI model 2000, ca. 600 ps FWHM, ~1.3 mJ per pulse) was also used.

2.3.3. Fourier transform infrared spectroscopy (FTIR)

Infrared spectra were recorded with a Nicolet Impact 400D FTIR spectrometer in transmittance mode by the use of KBr pellets. Spectra were recorded at 1.0 cm^{-1} resolution, in the range 4000–500 cm^{-1} as a ratio of 36 single-beam scans of the sample to the same number of background scans from air. Baseline corrections were introduced whenever needed. The original samples were diluted in KBr (about 2% w/w) and ground with the use of a agate mortar and pestle, to form a finely divided powder.

3. Results and discussion

3.1. UV-Vis. ground state diffuse reflectance and FTIR absorption spectra

Fig. 1a shows the ground state absorption spectra (n → π* transition only) of the inclusion complex of benzophenone and calix[6]arene, while Fig. 1b and c present similar data for silicalite and microcrystalline cellulose as hosts.

Remarkable differences can be observed in these three sets of spectra: in the calix[6]arene and silicalite cases a reasonably well defined vibronic structure is observed in the n → π* benzophenone absorption region which becomes non-structured and broad band in the cellulose case. A similar behaviour was observed by us [37] going from benzophenone deposited on the surface of microcrystalline cellulose to benzophenone entrapped within the cellulose polymer chains. As we recently also demonstrated the use of diffuse reflectance techniques [30], benzophenone included in calix[4]arene is in a less polar environment than in calix[8] and calix[6]arenes.

Fig. 2 shows a comparison of the 1 mol:1 mol inclusion complexes of benzophenone and calix[6]arene (curve 1), 250 μmol g^{-1} of benzophenone included within silicalite channels (curve 2) and also 500 μmol g^{-1} of benzophenone entrapped within cellulose polymer chains (curve 3).

The shift shown in Fig. 2 is well known and characteristic of the n → π* transition of benzophenone carbonyl group: polar and polar protic solvents promote hypsochromic shifts, due to the fact that the dipole moment of the carbonyl group in the ground state is larger than in the excited state. The energy level of the ground state is therefore more lowered by solvent interaction than the energy level of the excited state. The comparison of Fig. 2 suggests an increase of polarity in the environment of the guest ketone carbonyl group as going from calix[6]arene to silicalite and microcrystalline cellulose. This explains the deviation of the n → π* absorption band to the blue and the simultaneous broadening of the spectra with loss of vibronic resolution in the cellulose case.

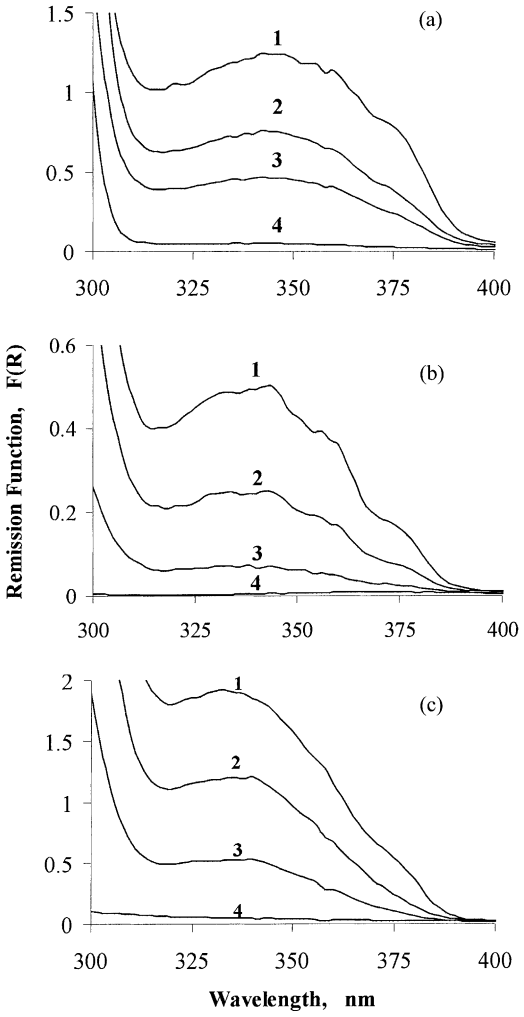

Fig. 1. (a) Remission function for benzophenone/calix[6]arene inclusion complexes with a molar ratio of 1:1, 1:2.5, 1:5 and also for the substrate curves 1–4, respectively. (b) Remission function for benzophenone/silicalite samples with concentrations of 100, 250, 500 μmol g^{-1} and also for the substrate curves 1–4, respectively. (c) Remission function for benzophenone/cellulose samples with concentrations of 150, 500, 1000 μmol g^{-1} and also for the substrate curves 1–4, respectively.

Table 1 presents data regarding the carbonyl stretching wavenumbers obtained from FTIR absorption spectra for samples of benzophenone/calix[6]arene, benzophenone/silicalite and benzophenone/cellulose. A comparison is made with microcrystals of benzophenone, where the carbonyl stretching band is located at 1651 cm^{-1} [30].

Fig. 3 shows data obtained for the samples of benzophenone with calix[6]arene, silicalite and cellulose in comparison with BZP microcrystals.

Benzophenone exhibits an extended conjugated system, resonance interactions being very important for the planar conformations of benzophenone in the microcrystals case. The more important they are, the weaker the C=O energy becomes as it assumes more single bond character. Inclusion of the ketone into the calixarene cavity, silicalite channels or cellulose polymer chain entrapment may promote deviations

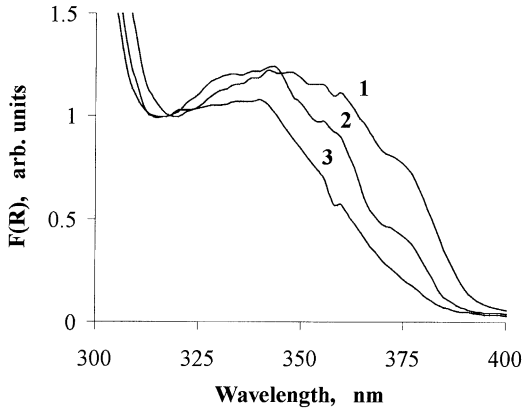

Fig. 2. Remission function (normalised at 320 nm) for benzophenone/calix[6]arene inclusion complex (molar ratio 1:1) curve 1 and also for benzophenone into silicalite (500 μmol g^{-1}) curve 2 and cellulose (450 μmol g^{-1}) curve 3, respectively.

Table 1
Carbonyl stretching band wavenumbers obtained from FTIR absorption spectra for samples of benzophenone/calix[6]arene inclusion complexes when compared with microcrystals of benzophenone, silicalite channel inclusion and cellulose entrapment

Microcrystals of BZP[a], $\nu_{C=O}$ (cm^{-1})	1651		
BZP/calix[6]arene (mol:mol)[a],	1:1	1:2.5	1:5
$\nu_{C=O}$ (cm^{-1})	1661	1662	1662
BZP/silicalite (μmol g^{-1})	500	250	100
$\nu_{C=O}$ (cm^{-1})	1671	1671	1672
BZP/cellulose (μmol g^{-1})	1500	1000	750
$\nu_{C=O}$ (cm^{-1})	1653	1653	1653

[a] Data from [30].

from planarity as reported previously for native and microcrystalline cellulose [43,44]. Decreasing resonance means increasing the energy of the C=O stretching mode due to the C=O double bond character enhancement (when compared with ketone microcrystals).

This effect is maximum for the silicalite case (inclusion into channels), and minimum in the cellulose case, where benzophenone molecules are almost as planar as in microcrystals of the ketone (Table 2). Clearly, calix[6]arene case is in an intermediate situation. These conformational restric-

Table 2
Phosphorescence emission lifetimes (half-life, longer components) for benzophenone/calix[6]arene inclusion complexes when compared with microcrystals of benzophenone and also with silicalite channel inclusion or cellulose entrapment of benzophenone

	Air equilibrated			Argon purged		
Microcrystals of BZP, τ_P (μs)[a]	35			37		
BZP/calix[6]arene (mol:mol)	1:1	1:2.5	1:5	1:1	1:2.5	1:5
τ_P (μs)[a]	40	35	35	40	35	35
BZP/silicalite (μmol g^{-1})	500	250	100	500	250	100
τ_P (μs)[a]	110	110	100	700	650	400
BZP/cellulose (μmol g^{-1})	1500	1000	750	1500	1000	750
τ_P (μs)[a]	70	75	75	70	75	75

[a] ±5%.

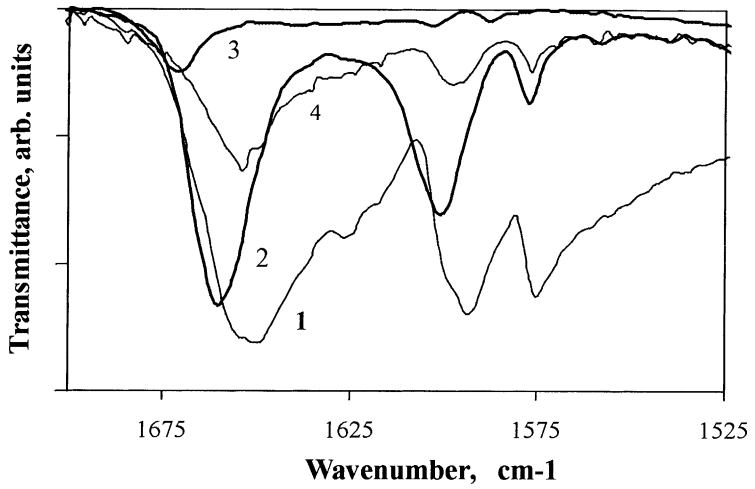

Fig. 3. Transmission FTIR absorption spectrum of microcrystals of benzophenone (curve 1) and of benzophenone/calix[6]arene inclusion complex (curve 2) with a 1:1 molar ratio in a KBr matrix. Curve 3 presents similar data for benzophenone/silicalite 500 μmol g^{-1} sample and curve 4 is for benzophenone/cellulose 750 μmol g^{-1} sample.

tions have an influence in the benzophenone phosphorescence emission intensity as we will show in the next paragraph.

3.2. Room temperature laser-induced phosphorescence

Fig. 4a shows the room temperature phosphorescence spectra of a 1 mol:1 mol inclusion complex of benzophenone and calix[6]arene while Fig. 4b and c present similar data for silicalite (250 μmol g^{-1}) and microcrystalline cellulose (1000 μmol g^{-1}) as hosts respectively. As an excitation source we used the short pulse (600 ps halfwidth) of a nitrogen laser pulse at 337 nm quite suitable to benzophenone time-resolved luminescence studies, due to its short duration. All time-resolved spectra presented in Fig. 4 were obtained with air equilibrated samples.

Spectra were also recorded for argon purged samples and were identical in spectral and intensity terms, within experimental error, for calix[6]arene and cellulose. For silicalite an increase of about one order of magnitude in the phosphorescence intensity was found with oxygen removal. In terms of the phosphorescence intensity, argon purged benzophenone/silicalite samples are about two orders of magnitude higher than for the two other hosts. Different lifetimes obtained are shown in Table 2.

A comparison of the emission decay from microcrystals of benzophenone [37,45] (complex decay, with an initial fast component followed by a longer component of $\tau_P \cong 35$ μs [45]) with the decay of benzophenone in the three hosts evidences several differences. The vibronic bands are different and the phosphorescence lifetimes vary from case to case (although after the initial fast component the decay becomes essentially mono-exponential in all cases of inclusion).

The insets of Fig. 4 show the decay curves obtained for the three hosts and Table 2 presents all the benzophenone decay parameters obtained in this work. The phosphorescence spectrum of benzophenone microcrystals exhibits a well defined vibrational structure. This structure still exists in the calixarene and cellulose cases. The benzophenone emission from the silicalite sample is less defined and the vibronic bands are broadened.

The decrease in the benzophenone lifetime going from silicalite to microcrystalline cellulose and to calix[6]arene is related to the rigidity of the host. Silicalite has a rigid crystalline structure composed by zig-zag channels intersecting other linear channels. In the intersection points probes have more space available than they have inside the elliptical channels where the largest internal dimension is about 5.6 Å. This heterogeneous environment justifies the broadening of the phosphorescence emission spectrum when compared with the other two hosts. Rigidity explains the very high phosphorescence lifetime obtained for this host, as a consequence of the decrease of the non-radiative mechanisms of deactivation. For calix[6]arene eight possible conformations exist [11,13] providing a greater structural flexibility (winged and hinged conformations) [11,19,23,30], therefore providing a less rigid environment when comparing with silicalite. For microcrystalline cellulose, entrapment within cellulose polymer chains also provides certain rigidity but not as much as silicalite.

In the calix[6]arene and in the cellulose cases, hydrogen abstraction reactions of benzophenone with the hosts and the consequent benzophenone radical formation occurs, as we will show in the next paragraph by the use of DRLFP technique. The more ketone radical is formed, the smaller lifetime for benzophenone phosphorescence emission was experimentally determined because photochemistry is competing with the radiative process of deactivation of the triplet state.

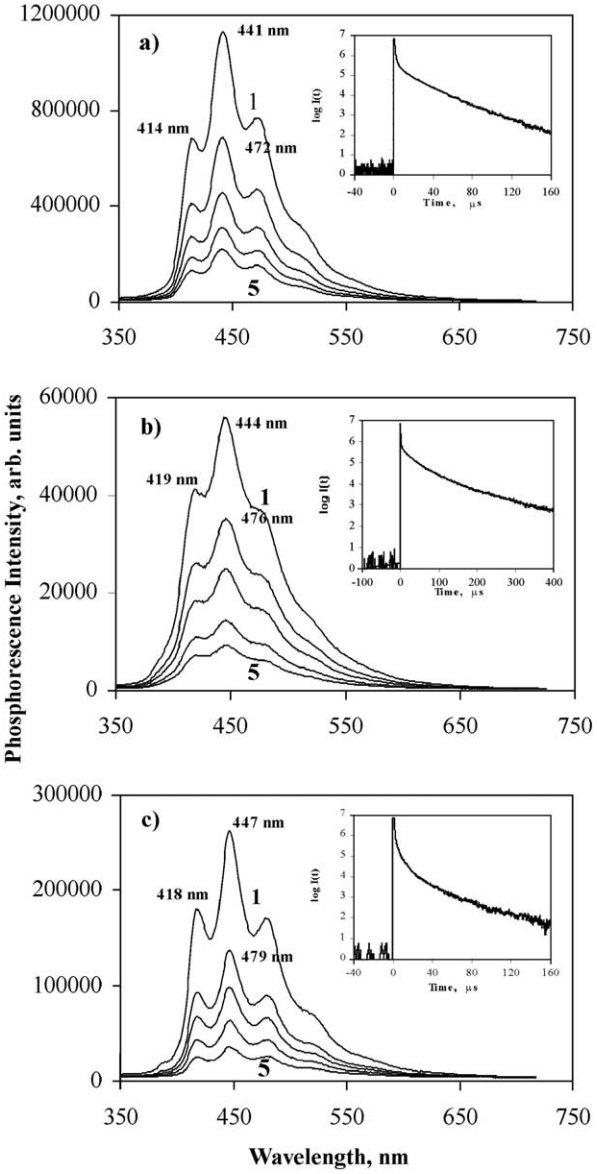

Fig. 4. Room temperature laser-induced phosphorescence emission spectra from an air equilibrated sample of (a) benzophenone/calix[6]arene inclusion complex (molar ratio 1:1). Curves 1, 2, 3, 4 and 5 were recorded 1, 25, 50, 75 and 100 μs after laser pulse. (b) Benzophenone/silicalite 250 μmol g^{-1} sample. Curves 1, 2, 3, 4 and 5 were recorded 1, 50, 100, 200 and 300 μs after laser pulse. (c) Benzophenone/cellulose 1000 μmol g^{-1} sample. Curves 1, 2, 3, 4 and 5 were recorded 1, 25, 50, 100 and 200 μs after laser pulse. The inset shows the phosphorescence time decay for each sample.

3.3. Diffuse reflectance laser flash photolysis

Time-resolved absorption spectra and decay kinetics of benzophenone onto powdered solid hosts were obtained by the use of DRLFP technique, developed by Wilkinson and Kelly [2,3]. In this study an intensified charged coupled device was used as detector, which allowed us to obtain time-resolved absorption spectra with nanometer resolution [30].

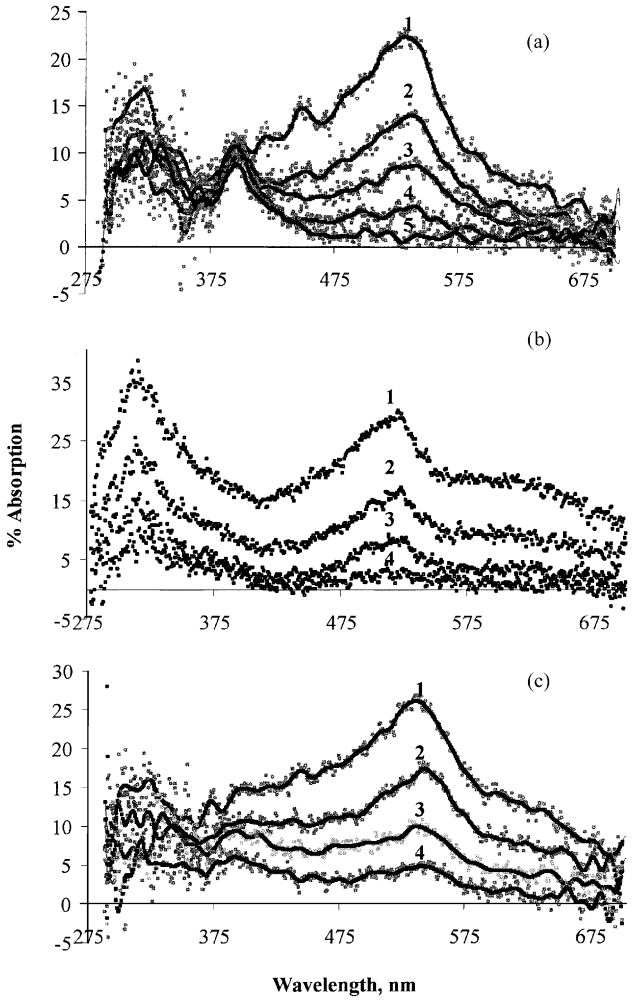

Fig. 5. (a) Time-resolved absorption spectra of benzophenone/calix[6]-arene inclusion complex (molar ratio 1:1). Curves 1, 2, 3, 4 and 5 were recorded 0.3, 1.0, 2.0, 5.0 and 50 μs after laser pulse. (b) Time-resolved absorption spectra of benzophenone/silicalite 250 μmol g^{-1} sample. Curves 1, 2, 3 and 4 were recorded 0.1, 10, 25 and 100 μs after laser pulse. (c) Time-resolved absorption spectra of benzophenone/cellulose 1500 μmol g^{-1} sample. Curves 1, 2, 3 and 4 were recorded 0.1, 1.0, 5.0 and 20 μs after laser pulse.

Fig. 5a shows the time-resolved absorption spectra of benzophenone/calix[6]arene inclusion complex (molar ratio 1:1) and Fig. 5b and c shows similar data for benzophenone/silicalite and benzophenone/cellulose host/guest systems.

Transient absorption spectra of inclusion complexes of *p-tert*-butylcalix[n]arenes ($n = 4, 6, 8$) with benzophenone provide evidence for major triplet formation in the calix[4]arene case [30]. In this case the time-resolved absorption spectra peaks at about 525 nm both initially and at longer time scales, showing that the absorption is mainly due to the benzophenone triplet excited state.

The ketyl radical of benzophenone becomes evident in the calix[6]arene case as Fig. 5a clearly shows. In these spectra, even at initial times (0.3 μs after laser pulse) a 550 nm peak

is present, characteristic of the benzophenone ketyl radical absorption. At about 400 nm the well known absorption band of the phenoxyl radical can also be observed. Therefore, the calix[6]arene acts as a hydrogen atom donor towards the excited aromatic ketone. The same behaviour was detected for the benzophenone/calix[8]arene inclusion complex [30]. Direct excitation of the three calixarenes without the guest also evidence the phenoxyl radical formation of the calixarenes, as reported before [30].

The fact that no benzophenone ketyl radicals were formed in the calix[4] case and that evidence for ketyl radical formation was found in the calix[6] and calix[8] cases is related with the increase of the internal space of the cavity enabling conformations suitable for the hydrogen abstraction to occur [30].

Inside the silicalite channels benzophenone finds no suitable hydrogen atom donor and the triplet–triplet $T_1 \rightarrow T_2$ and $T_1 \rightarrow T_3$ transient absorptions of this aromatic ketone were observed and identified, peaking at 520 and 320 nm, respectively. Those absorption maxima are similar to those determined for benzophenone transient absorption in solvents such as benzene or acetonitrile [46].

Microcrystalline cellulose varies as a host depending on the solvent used for sample preparation. Benzophenone can be entrapped within the natural polymer chains whenever ethanol (or other polar protic solvents) is used for sample preparation or on the surface of the substrate if solvents such as dichloromethane or benzene are used. In the former case photochemical reactions occur with ketyl radical formation, as Fig. 5c clearly shows, while in the latter benzophenone microcrystals behaviour (triplet–triplet transient absorption) is detected [37]. These transient absorption data have shown us that photochemistry is competing with phosphorescence emission in the deactivation of the triplet excited state of benzophenone.

4. Conclusions

Inclusion of benzophenone into different hosts results in significative changes both in ground-state absorption spectra as well as time-resolved emission and absorption spectra.

In the calix[6]arene case the probe is in a hydrophobic and constrained environment, which exhibits a small polarity. This host allows interactions of the carbonyl group of the ketone with the hydroxyl groups of the calixarene and, as result, ketyl radical formation was detected.

Silicalite as a host provides the most rigid environment for the aromatic ketone, the internal cavities being zig-zag channels which intersect. Therefore, inclusion sites are non-homogeneous and the phosphorescence emission spectrum reflects this fact: the vibronic bands are broadened, when compared both with calix[6]arene and cellulose.

For benzophenone entrapped into cellulose polymer chains (ethanol swelling of cellulose), and in agreement with previous work from our group [37], clear evidence was found for benzophenone ketyl formation which peaks at 550 nm.

Benzophenone phosphorescence is maximum in the most rigid crystalline material, silicalite (in spite of the fact that the ketone is more distorted from planarity), which is at the same time the most inert material from the photochemical point of view. Both in cellulose and calix[6]arene the photochemistry is significant, the difference being that calix[6]arene is less rigid due to the conformations it exhibits.

Acknowledgements

This work was partially presented at the Frank Wilkinson Symposium, June 2001, Loughborough, UK, as an oral communication. Equipment was financed by project Praxis/P/Qui/10023/98. The authors thank ICCTI/CAPES for financial support. ASO thanks FCT for a Post-Doctoral fellowship (SFRH/BPD/3650/2000).

References

[1] L.F. Vieira Ferreira, Química 72 (1999) 28;
A.M. Botelho do Rego, L.F. Vieira Ferreira, in: H.S. Nalwa (Ed.), Handbook of Surfaces and Interfaces of Materials, vol. 2, Academic Press, New York, Chapter 7, 2001.
[2] F. Wilkinson, G.P. Kelly, in: M. Anpo, T. Matsuara (Eds.), Photochemistry on Solid Surfaces, Elsevier, Amsterdam, 1989, p. 31.
[3] F. Wilkinson, G.P. Kelly, in: J.C. Scaiano (Ed.), Handbook of Organic Photochemistry, vol. 1, CRC Press, Boca Raton, 1989, p. 293.
[4] R.J. Hurtubise, Anal. Chim. Acta 351 (1997) 1.
[5] C.D. Gutshe, Calixarenes, Royal Society of Chemistry, Cambridge, UK, 1989;
C.D. Gutshe, Calixarenes revisited, Monographs in Supramolecular Chemistry, Royal Society of Chemistry, Cambridge, UK, 2000.
[6] L. Mandolini, R. Ungaro (Eds.), Calixarenes in Action, Imperial College Press, London, 2000.
[7] J. Vicence, V. Böhmer (Eds.), Calixarenes, Kluwer Academic Press, Dordrecht, 1991.
[8] V. Jacques, J.McB. Harrowfield, Calixarenes 50th Anniversary: Commemorative Issue, Kluwer Academic Publishers, Dordrecht, 1995.
[9] C.D. Gutsche, Aldrichim. Acta 28 (1995) 3.
[10] V. Bohmer, Angew. Chem. Int. Ed. Engl. 34 (1995) 713.
[11] L.J. Bauer, C.D. Gutsche, J. Am. Chem. Soc. 107 (1985) 6063;
C.D. Gutsche, L.J. Bauer, J. Am. Chem. Soc. 107 (1985) 6052.
[12] P.D. Beer, P.A. Gale, D.K. Smith, Supramolecular Chemistry, Oxford University Press, Oxford, 1999.
[13] A. Ikeda, S. Shinkai, Chem. Rev. 97 (1997) 1713.
[14] Y. Liu, B.H. Han, Y.T. Chen, J. Org. Chem. 65 (2000) 6227.
[15] J.L. Atwood, G.A. Koutsantonis, C.L. Raston, Nature 368 (1994) 229.
[16] S. Shinkai, A. Ikeda, Pure Appl. Chem. 71 (1999) 275;
T. Suzuki, K. Nakashima, S. Shinkai, Chem. Lett. (1994) 669.
[17] G.J. Lumelta, R.D. Rogers, G. Aravamudan, Calixarenes for Separations, Amer. Chem. Soc. Pub., New York, 2000.
[18] R. Perrin, R. Lamartine, M. Perrin, Pure Appl. Chem. 65 (1993) 1549.
[19] M. Lazzarotto, F.F. Nachtigal, F. Nome, Quimica Nova 18 (1995) 444.

[20] R. Ungaro, A. Arduini, A. Casnati, A. Pochini, F. Ugozzoli, Pure Appl. Chem. 68 (1996) 1213.
[21] P. Mnuk, L. Feltl, J. Chromatogr. 696 (1995) 101.
[22] N. Megson, Osterr. Chem. Z. 54 (1953) 317;
J. Cornforth, P. Hart, G. Nicholls, R. Rees, B. Stock, J. Pharmacol. 10 (1955) 73.
[23] T.-M. Liang, K.K. Laali, Chem. Ber. 124 (1991) 2637.
[24] K. Araki, K. Akao, K. Otsuka, K. Nakashima, F. Inokuchi, S. Shinkai, Chem. Lett. (1994) 1251.
[25] I. Alam, C.D. Gutsche, J. Org. Chem. 55 (1990) 4487.
[26] C.D. Gutsche, I. Alam, Tetrahedron 44 (1988) 4689.
[27] C.H. Tung, H.F. Ji, J. Chem. Soc., Perkin Trans. 2 (1997) 185.
[28] S. Shinkai, K. Araki, O. Manabe, J. Chem. Soc., Chem. Commun. 3 (1988) 187.
[29] A.F. Danil de Namor, R.G. Hutcherson, F.J. Sueros Velarde, M.L. Zapata-Ormachea, L.E. Pulcha Salazar, I. Al Jammaz, N. Al Rawi, Pure Appl. Chem. 70 (1998) 769.
[30] L.F. Vieira Ferreira, M.R. Vieira Ferreira, A.S. Oliveira, T.J.F. Branco, J.V. Prata, J.C. Moreira, Phys. Chem. Chem. Phys. 4 (2002) 204–210.
[31] M. Barra, K.A. Agha, Supramol. Chem. 10 (1998) 91.
[32] Y. Shi, Z. Zhang, J. Chem. Soc., Chem. Commun. (1994) 375;
Y. Shi, D. Wang, Z. Zhang, J. Photochem. Photobiol. 91 (1995) 211.
[33] F. Huang, J. Yang, A. Hao, X. Wu, R. Liu, Q. Ma, Spectrochim. Acta A 57 (2001) 1025.
[34] J.L. Bourdelande, J. Font, R. González-Moreno, S. Nonell, J. Photochem. Photobiol. A 115 (1998) 69;
J.L. Bourdelande, J. Font, R. González-Moreno, J. Photochem. Photobiol. A 94 (1996) 215.
[35] J. Vincens, Mol. Cryst. Liq. Cryst. 187 (1990) 115.
[36] E.C. Flaningen, J.M. Bennet, R.W. Grose, R.L. Patton, R.M. Kirchner, J.V. Smith, Nature 271 (1978) 512;
G.M.W. Shultz-Sibbel, D.T. Gjerde, C.D. Chriswell, J.S. Fritz, W.E. Colleman, Talanta 29 (1982) 447;
D.M. Bibby, N.B. Millestone, L.P. Aldridge, Nature 280 (1979) 664.
[37] L.F. Vieira Ferreira, J.C. Netto-Ferreira, I. Khmelinskii, A.R. Garcia, S.M.B. Costa, Langmuir 11 (1995) 231.
[38] L.F. Vieira Ferreira, M.R. Freixo, A.R. Garcia, F. Wilkinson, J. Chem. Soc., Faraday Trans. 88 (1992) 15;
L.F. Vieira Ferreira, A.R. Garcia, M.R. Freixo, S.M.B. Costa, J. Chem. Soc., Faraday Trans. 89 (1993) 1937.
[39] A.S. Oliveira, M.B. Fernandes, J.C. Moreira, L.F. Vieira Ferreira, J. Bras. Chem. Soc. 13 (2002) 254.
[40] L.F. Vieira Ferreira, M.J. Lemos, M.J. Reis, A.M. Botelho do Rego, Langmuir 16 (2000) 5673.
[41] L.F. Vieira Ferreira, A.S. Oliveira, J.C. Netto-Ferreira, in: A. Kotyk (Ed.), Fluorescence Microscopy and Fluorescence Probes 3, Espero Publishers, Prague, 1999, p. 199.
[42] L.F. Vieira Ferreira, J.C. Netto-Ferreira, S.M.B. Costa, Spectrochim. Acta A 51 (1995) 1385.
[43] L. Ilharco, A.R. Garcia, J.L. Silva, M.J. Lemos, L.F. Vieira Ferreira, Langmuir 13 (1997) 3787.
[44] L. Ilharco, A.R. Garcia, J.L. Silva, L.F. Vieira Ferreira, Langmuir 13 (1997) 4126.
[45] F. Wilkinson, C.J. Willsher, Chem. Phys. Lett. 104 (1984) 272.
[46] I. Carmichael, G.L. Hug, J. Phys. Chem. Ref. Data 15 (1986) 1.